Waste and Biomass Valorization
https://doi.org/10.1007/s12649-022-01679-z

ORIGINAL PAPER

Bio-composite Films Based on Alginate and Rice Husk Tar Microparticles Loaded with Eugenol for Active Packaging

María E. Taverna[1,2] · Carlos A. Busatto[1] · Paula J. Saires[3] · Melisa P. Bertero[3] · Ulises A. Sedran[3] · Diana A. Estenoz[1]

Received: 26 June 2021 / Accepted: 3 January 2022

Abstract

This work focused on the valorization of tar derived from rice husk pyrolysis as a precursor of matrices for the encapsulation of active principles. In this regard, the development of novel films based on alginate and eugenol-loaded tar microparticles with suitable mechanical properties and antibacterial activity was studied. Tar microparticles loaded with eugenol were incorporated into sodium alginate films and the effect on the mechanical, thermal and humidity resistance properties were determined, as well as the antimicrobial activity. Films with different crosslinking degrees were also prepared using $CaCl_2$, and the eugenol controlled release profiles were evaluated. Crosslinked films exhibited improved mechanical and humidity resistance properties, as well as a lower release rate of eugenol in water. The antimicrobial studies showed that eugenol-loaded films present a higher antimicrobial activity against *Staphylococcus aureus*. Alginate/eugenol-loaded tar microparticles composites showed an enhancement of antibacterial properties and suitable physical characteristics to be used in active packaging applications.

Graphical Abstract

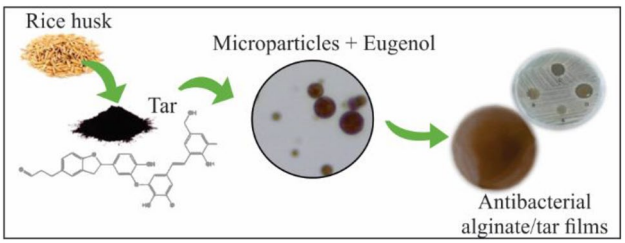

Keywords Alginate films · Active packaging · Pyrolysis · Tar · Eugenol

Statement of Novelty

The novelty of this article involves the valorization of rice husk pyrolytic tar by means of the preparation of tar microparticles encapsulating eugenol and their inclusion in alginate films to develop active packaging materials.

Introduction

In the last years, the food industry has generated new demands due to the growing consumer interest in fresh or minimally processed food, free of synthetic preservatives

✉ Diana A. Estenoz
destenoz@santafe-conicet.gov.ar

1 Instituto de Desarrollo Tecnológico para la Industria Química, INTEC (UNL - CONICET), 3000 Santa Fe, Argentina

2 UTN Facultad Regional San Francisco, Av. de la Universidad 501, 2400 San Francisco, Córdoba, Argentina

3 Instituto de Investigaciones en Catálisis y Petroquímica "Ing. José Miguel Parera", INCAPE (UNL-CONICET), Colectora Ruta Nac. 168 Km. 0, 3000 Santa Fe, Argentina

Published online: 29 January 2022

and with extended shelf life and controlled quality. To fulfil these requirements, the development of active packaging appears as a promising technology to improve food preservation, by interacting with the food product and/or the packaging headspace [1]. Among several additives that can be included into the packaging matrix, the use of antimicrobials from natural origin is becoming an interesting alternative due to the potential health issues associated with synthetic preservatives.

Eugenol(4-allyl-2-methoxyphenol) is a phenolic compound mainly present in essential oils, such as clove, cinnamon, and nutmeg. This naturally occurring compound has been widely investigated for different applications in the food, pharmaceutical, cosmetic and dental care industry due to its antimicrobial, antioxidant and analgesic properties [2]. Although eugenol exhibits a broad-spectrum antibacterial activity, its application in the food industry is usually limited by its high volatility and sensitivity to oxygen, light and heat [3]. To overcome this problem, the incorporation of eugenol into a polymer matrix has been proposed as an efficient alternative to produce active packaging items with controlled release behaviour. Several antibacterial films incorporating eugenol were reported, including starch [3, 4], linear low density polyethylene [5], poly(3-hydroxybutyrate-co-3-hydroxyvalerate) [6], chitosan and sodium alginate [7]; and gelatine films [8]. Among them, antibacterial films made of polymers from natural resources (i.e., polysaccharides, proteins and lipids) are preferred to petroleum-based polymers due to their biodegradable, renewable and safety characteristics. In this sense, sodium alginate is an attractive option to encapsulate eugenol.

In turn, microencapsulation technology is widely used in the pharmaceutical, agrochemical, and food industries [9]. The encapsulation of an active compound may limit its losses during film processing while also helping to modulate its release kinetics from the packaging material. In this direction, products obtained from lignocellulosic biomass represent a sustainable choice for the microencapsulation of active compounds into packaging materials. In particular, thermochemical processes such as biomass pyrolysis or gasification are interesting methods to obtain potential value-added products. These processes produce liquids, which can be easily separated into two fractions according to their water solubility. The water insoluble fraction (tar) exhibits a very complex composition [10] and is more viscous and denser than the water-soluble fraction, usually named bio-oil.

Tar from biomass pyrolysis is mainly composed of monophenol derivatives such as phenol, guaiacol, and syringol, and some aromatic oligomers, including stilbene, phenyl coumaran and resinol [11]. Even though bio-oils were extensively used as fuels or for the separation of high-value chemicals [12, 13], the valorization of tar has been barely explored [14]. For example, tar was used as partial replacement of phenol in phenolic resins [15] and asphalt production [16]. Recently, pyrolytic tar was used for the synthesis of microparticles [17]. Tian et al. (2020) [17] reported the synthesis of alginate microspheres containing sawdust tar for adsorption applications. So far, the use of tar for the microencapsulation of active compounds has not been reported. In addition, few studies have been conducted on the antimicrobial activity of sodium alginate combined with essential oils [18].

The aim of this work is to investigate the use of rice husk tar for the microencapsulation of eugenol in alginate films as potential active packaging materials. The preparation of eugenol-loaded tar microparticles was performed by the solvent evaporation technique, and microparticles were used for the fabrication of antimicrobial sodium alginate films. The functional properties of the composite films were evaluated, including thermal, mechanical and barrier properties, as well as the eugenol-controlled release behaviour and the antimicrobial activity against foodborne pathogens.

Experimental

Materials

The following reagents were used as received: $CaCl_2$ (Sigma-Aldrich, Germany), sodium alginate (Todo Drogas, Argentina), polyvinyl alcohol (PVA) (205 kDa, 87.7% hydrolyzed, Sigma Aldrich, Germany), eugenol (Sigma Aldrich, Germany), methylene chloride (Cicarelli, Argentina). Tar was obtained from the pyrolysis of rice husk biomass. To this effect, rice husk was fed at a rate of 0.8–1 kg min^{-1} to a pilot scale downdraft reactor operated at 485 °C with air flow of 16 L min^{-1}. The experiment was performed during 5 h. Tar was collected from the condenser in the pilot unit. Tar yield, calculated on a dry biomass basis, was 1.8 wt%. Deionized water was used to prepare all solutions.

Characterization of Tar Obtained from Rice Husk Pyrolysis

The characterization of tar included the following determinations: (a) moisture content by Karl-Fischer analysis; (b) total carbon (C), hydrogen (H), sulfur (S) and nitrogen (N) contents by elemental analysis; and (c) molar mass by size exclusion chromatography (SEC). For the SEC analysis, a Waters (Massachusetts, USA) Model 1525 chromatograph with an automatic injector (Waters 717plus) was used. The equipment was fitted with a set of Waters Styragel HR 4 E (7.6 × 300 mm) columns and a differential refractometer detector (Waters 2414). The carrier solvent was THF at 1 mL min^{-1} and the system was operated at 25 °C. The

sample was dissolved in 0.25 mL THF with a nominal concentration of 1 mg mL^{-1}. Injection volumes were 200 µL. A set of 9 poly(ethylene glycol) standards (Service GmbH) were used for the calibration.

Preparation of Tar Microparticles

Tar microparticles were prepared by the solvent extraction/evaporation technique. To this effect, approximately 60 mg of tar were dispersed and sonicated in 6 mL of dichloromethane (DCM). Then, the dispersion was filtered with a 0.45 µm nylon syringe filter (Microclar, Argentina) to remove undissolved tar. Eugenol standard (60 mg) was added to the filtered solution (6 mL). This solution was slowly dropped onto an aqueous phase (17 mL of 2% w/v PVA solution) under continuous stirring at 500 rpm using a homogenizer (Kinematica Polytron PT 2500e, Switzerland). Then, 10 mL of the PVA solution was added to the emulsion and the stirring was continued for 30 min. The organic solvent was evaporated under vacuum on a rotary evaporator (Büchi EL 130, Germany) for 1 h at room temperature. Solid microparticles were collected by centrifugation (Heal force 15/R, China) at 2000 rpm for 3 min. Microspheres were dried at 40 °C and stored until further analysis.

Microparticle Size Distribution

Optical micrographs were obtained by observation of microparticle suspensions under an optical microscope (DM 2500M, Leica, Germany) coupled with a camera (DFC 290 HD, Leica). Approximately 300 microparticles per sample were measured for the determination of the particle average size and size distribution, using image processing software.

Eugenol Entrapment

Eugenol encapsulation in tar microparticles was determined indirectly. Non-entrapped eugenol was quantified in the supernatant of microparticle suspensions after their preparation. To this effect, solid microparticles were collected by centrifugation at 2000 rpm for 2 min and eugenol concentration in the aqueous supernatants was quantified using a UV–Vis spectrophotometer (Perkin Elmer Lambda 25) at 279 nm. The calibration curve ($R^2 = 0.9984$) was performed in the 0–100 mg L^{-1} range. Five eugenol standard solutions in water were used for calibration. The assay was run in duplicate. Eugenol entrapment was calculated as follows:

$$En(wt\%) = \frac{mi - ms}{mp} \times 100$$

where *mi* and *ms* are the initial mass of eugenol and the mass of eugenol determined in the supernatant of microparticles after centrifugation, respectively and *mp* is the total mass of microparticles.

Preparation of Sodium Alginate and Sodium Alginate/Tar Microparticles Films

First, a 2.0 wt% sodium alginate solution was prepared in distilled water at 60 °C until complete dissolution. To plasticize the films, glycerol (1 wt%) was added to the solution. Film compositions are presented in Table 1. Sodium alginate and sodium alginate/tar microparticles films (named Alg and Alg/Tar, respectively) were casted on silicone molds (6 cm diameter) and dried in an oven at 60 °C for 24 h. Then, the films were removed and kept in a desiccator until further analysis. Ionically crosslinked alginate films were also prepared by $CaCl_2$ treatment. Dried films were embedded in $CaCl_2$ solutions at different concentrations, and the resulting films were named according to the crosslinker mass percentage with respect to the polymer (Table 1). Finally, the films were washed with water and dried in an oven at 40 °C for 24 h.

Films Characterization

The characterization of sodium alginate and sodium alginate/tar microparticles films included the following determinations: (a) moisture and water solubility tests by gravimetric analysis; (b) functional groups by Fourier-transform infrared spectroscopy (FTIR); (c) thermal stability by thermogravimetric analysis (TGA); (d) opacity by UV–Vis spectroscopy; (e) surface hydrophilicity by contact angle, (f) elastic modulus by dynamic mechanical analysis (DMA), and (g) film morphology by optical microscopy.

Moisture content was determined according to the gravimetric method reported by Aadil et al. (2017) [19]. The sample was dried in an oven at 105 °C until constant weight.

For the water solubility tests, the films were weighted and incubated in 50 mL of water for 24 h at room temperature. Then, the solution was filtered through a filter paper under vacuum to recover the remaining film, which was

Table 1 Composition of sodium alginate and sodium alginate/tar microparticles films

	Alginate (g)	$CaCl_2$ (g)	Tar (g)
Alg	0.10	–	–
Alg + $CaCl_2$(20%)	0.10	0.02	–
Alg + $CaCl_2$(30%)	0.10	0.03	–
Alg/Tar	0.10	–	0.01
Alg/Tar + $CaCl_2$(20%)	0.10	0.02	0.01
Alg/Tar + $CaCl_2$(30%)	0.10	0.03	0.01

dried at 105 °C for 24 h and weighted. Solubility in water was determined according to Aadil et al. (2016) [19].

The characteristic functional groups of the films were investigated by FTIR. A 45° trapezoidal (80 × 10 × 4 mm) ZnSe crystal was used, providing 10 internal reflections at the liquid/crystal interface. The cell was mounted onto an ATR attachment (Pike Technologies) inside the sample compartment of the FTIR spectrometer (ThermoElectron, Nicolet 8700 with a cryogenic MCT detector).

TGA analyses were performed using a thermo-gravimetric analyser (Q500 TA instrument) under a nitrogen atmosphere at a flow rate of 80 mL min^{-1}. Film samples (about 5 mg) were heated from 40 to 600 °C at a heating rate of 10 °C min^{-1}.

Film opacity was determined using a spectroscopic method. Film samples were directly placed in a UV–vis spectrophotometer (Perkin Elmer Lambda 25) test cell. The absorbance spectrum of the sample was measured at 600 nm. Film opacity was defined as the ratio of the absorbance at 600 nm and the film thickness. Measurements were performed by triplicate for each sample.

Samples were submitted to a contact angle analysis in a Point Grey camera (BFLY-PGE-05S2M-CS model) with Edmund Optic #68-678 lens in order to determine surface hydrophilicity. Measurements were performed on evaporative plates at room temperature by deposition of ultrapure water droplets of 30 µL each, with an average flow rate of 500 µL s^{-1}.

DMA was performed to determine the elastic modulus of films. To this effect, films of 0.1 mm thick were analysed in tensile mode at different frequencies (0–100 Hz) with a 0.5% strain, using Q800 DMA equipment from TA Instruments.

Optical images of sodium alginate films incorporating tar microparticles were obtained following the procedure described in section 'Microparticle Size Distribution'.

Eugenol Release Assays

The controlled release behaviour of eugenol from tar microparticles and composite films was evaluated in aqueous medium [4]. To this effect, approximately 10 mg of eugenol-loaded microparticles were dispersed in 25 mL of ultrapure water and incubated at 25 °C. A similar procedure was followed for sodium alginate films containing approximately 10 mg of eugenol-loaded microparticles. Samples of 1 mL were taken at predetermined times and replaced with an equal volume of ultrapure water. Eugenol concentration in samples was quantified following the UV–Vis technique described in section 'Eugenol Entrapment'. The experiments were performed in duplicate.

Antimicrobial Activity of Films

Sodium alginate films incorporating eugenol-loaded microparticles were assayed for antimicrobial activity against *Escherichia coli* (ATCC 25922) and *Staphylococcus aureus* (ATCC 6538) as described elsewhere [20]. Inhibition halos against *E. coli* and *S. aureus* were evaluated by a disk diffusion method. Briefly, samples of film disks (6 mm diameter) were placed onto the surface of agar plates seeded with 10^4 CFU mL^{-1} of 16 ± 2 h grown microorganisms. Alginate films with and without non-loaded tar microparticles were also assayed as negative controls. After incubating the plates at 37 °C for 18 ± 2 h, the antimicrobial activity was evaluated by measuring the clear zone of growth inhibition for the active film and compared with the negative controls.

Statistical Analysis

The analysis of variance (ANOVA) with a confidence level of 95% was employed in order to perform the statistical analysis of the data obtained in the following tests: moisture content, water solubility, opacity, and contact angle. To this effect, a 2 × 2 factorial design was implemented using the free software R version 4.1.1. The selected factors were TAR and $CaCl_2$ content in the films.

Results and Discussion

Characterization of Tar Obtained from Rice Husk

Table 2 summarizes the physicochemical and molecular properties of rice husk tar.

A broad molar mass distribution with a high number of low molecular weight molecules was measured. Prauchner et al. (2001) [21] reported similar results for eucalyptus tar pitches. See the molar mass distribution in SI.

Table 2 Characterization of rice husk tar

Physicochemical properties	
% Moisture	12.1
% C, O, H, N	62.8, 28.8, 6.3, 2.1
Molecular properties	
$\overline{M}_w$(g mol^{-1})	708
$\overline{M}_n$(g mol^{-1})	329
Dispersity	2.15

Characterization of Tar Microparticles

Figure 1 shows a micrograph of tar microparticles, which exhibit a spherical morphology with a mean particle size of 14.95 ± 6.61 µm. The particle size distribution is also shown in Fig. 1, and it seems to fit a normal Gaussian distribution function with a confidence level greater than 95%. Eugenol entrapment in tar microparticles was 8.82 ± 3.92 wt%. In literature, there are different eugenol loadings reported [22]. In general, low entrapment values are attributed to the high solubility of eugenol in water when it is added to the aqueous phase during the microparticle synthesis [22].

Preparation and Characterization of Sodium Alginate and Sodium Alginate/Tar Microparticles Films

The moisture content and water solubility determinations of polymeric films are presented in SI (see Fig. S2).

The moisture content of polymeric films was around 15%, which was similar for all samples. The statistical analysis showed that there are not significant differences in films with or without tar ($p = 0.089 > 0.05$). This result was not affected by the crosslinking degree of sodium alginate or the addition of tar microparticles, probably due to the high sodium alginate content of films and the significant hydrophilic properties of alginate and glycerol, which can form hydrogen bonds with water molecules [19]. However, a slight decrease in moisture content was observed for films containing tar microparticles and with a higher crosslinking degree of sodium alginate ($p = 4.17 \times 10^{-5} < 0.05$), indicating a decreased water uptake due to the presence of hydrophobic tar microparticles and a more crosslinked polymer network.

Regarding the solubility tests, it can be seen that sodium alginate films without $CaCl_2$ treatment (Alg, Alg/Tar) were completely soluble after 24 h. This observation is in accordance with the results reported by Aadil et al. (2017) [19] in similar experimental conditions. As expected, the solubility of films was significantly affected by the crosslinking degree ($p = 2.45 \times 10^{-7} < 0.05$), but it did not change when tar microparticles were incorporated ($p = 0.123 > 0.05$). High water solubility values are a sign of low water resistance, which is an important parameter for commercial applications. However, this is a case-by-case decision depending on the purpose of application [23].

The incorporation of tar microparticles into sodium alginate films resulted in higher UV light absorption capacity (Fig. 2) and it was confirmed by statistical analysis that showed significant differences for films with or without tar ($p = 0.09 < 0.05$). This effect is due to the chromophore nature of tar, which is similar to that of lignin [19]. In addition, the transparency of films was affected with the incorporation of $CaCl_2$ ($p = 2.61 \times 10^{-5} < 0.05$), probably due to refractive index changes associated to the crosslinked domains. According to Michelin et al., (2020) [23], darkening of films can be an issue since most consumers prefer transparent packaging. However, for some products susceptible to degradation by UV exposure, such as cheese and

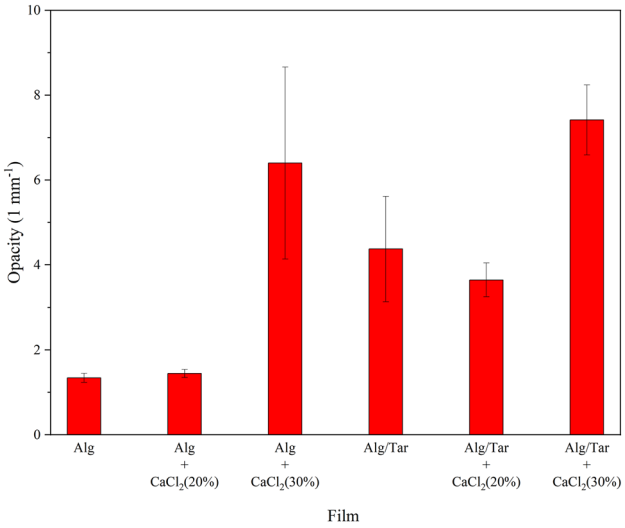

Fig. 2 Opacity of sodium alginate films with and without the addition of tar microparticles

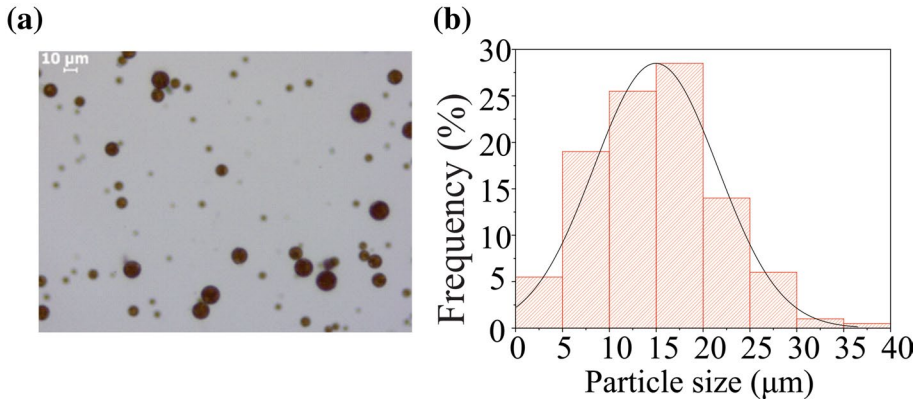

Fig. 1 **a** Optical images of tar microparticles; and **b** Particle size distribution

Table 3 Thermogravimetric analysis parameters

Sample	$T_{10\%}$ (°C)	Char (%)	Maximum degradation temperature (°C)
Alg	122	25.17	207
Alg + $CaCl_2$(20%)	159	28.61	210
Alg + $CaCl_2$(30%)	179	35.18	216
Alg/Tar	77	27.06	209
Alg/Tar + $CaCl_2$(20%)	155	27.10	217
Alg/Tar + $CaCl_2$(30%)	182	27.17	207

Table 4 Elastic modulus of the different films

Sample	E′ (MPa)*
Alg	1400
Alg + $CaCl_2$(20%)	3002
Alg + $CaCl_2$(30%)	2500
Alg/Tar	1775
Alg/Tar + $CaCl_2$(20%)	2250
Alg/Tar + $CaCl_2$(30%)	2300

*At 100 Hz

minimally processed vegetables suffering from lipid oxidation or colour change, opacity can be an advantage.

The main parameters of the thermogravimetric analyses are summarized in Table 3. Additional information of TGA and DTG are reported in SI (see Fig. S3).

According to the thermograms, three degradation zones can be identified. The first zone is related to moisture content. The second zone is attributed mainly to glycerol and alginate degradation [19, 23], in accordance with Aadil et al. (2017) [19]. Finally, the third zone is associated with tar degradation, as it presents an aromatic structure. The addition of $CaCl_2$ produces a slight increase in maximum degradation temperature. Char content at 600 °C increases after $CaCl_2$ treatment and with the incorporation of tar microparticles. These results indicate that the incorporation of tar and the crosslinking effect of $CaCl_2$ could improve the thermal stability of the films [24].

Table 4 presents the elastic modulus obtained in DMA analysis.

The storage modulus (E′) is a measure of the elastic response of the material to a given load. Alginate film without $CaCl_2$ (Alg) exhibited the lowest E′ compared to crosslinked or tar microparticles-containing films. The rigid aromatic structure of tar is associated with higher values of E′ [25]. However, no significant increase in E′ was observed for Alg/Tar, Alg/Tar + $CaCl_2$(20%), and Alg/Tar + $CaCl_2$(30%) films probably due to the high alginate:tar ratio in film compositions.

The incorporation of tar microparticles into alginate films treated with different $CaCl_2$ concentrations [Alg/Tar, Alg/Tar + $CaCl_2$(20%), and Alg/Tar + $CaCl_2$(30%)] resulted in a homogeneous distribution of tar microparticles in sodium alginate-based films (Fig. 3a–c). In addition, films showed flexibility, ease handling, and a non-sticky characteristic (Fig. 3d).

ATR-FTIR analysis for the different film compositions did not reveal important structural modifications (Fig. 4).

The main bands related to sodium alginate are 2925, 1736, 1562, 1481 and 1105 cm^{-1}, attributed to O–H, C–H, COO– (asymmetric), COO– (symmetric), and C–O stretching vibrations, respectively [19]. The skeletal vibrations of six membered (pyranose) rings of alginate at 956 cm^{-1} [19] are overlapped with a C–H out of plane vibration of tar. There are no differences in the absorbance intensity. The band at 797 cm^{-1} is associated to α C1 –H deformation vibration for alginate [26] and to C–C vibration for tar. No differences were revealed in the absorbance intensities for both spectra. The band at 3363 cm^{-1} could be attributed to the presence of a phenolic OH [10], and it is overlapped with the band corresponding to alcoholic groups OH from alginate [19]. In film spectra, the O–H bands of sodium alginate can be identified as a consequence of intermolecular interactions [19]. These interactions are lower in films treated with $CaCl_2$.

Contact angle values for the different films are presented in Fig. 5.

Contact angle measurements showed a lower energy surface with the incorporation of tar ($p = 8.46 \times 10^{-11} < 0.05$). The contact angle increase of tar-containing films is due to the aromatic structure of tar, which makes the film surface more hydrophobic [25]. In addition, an increase in the contact angle values of films treated with $CaCl_2$ was observed, which is due to the lower water uptake capacity of crosslinked films. It is important to note that ANOVA showed significant statistical differences ($p = 1.2 \times 10^{-6} < 0.05$) in the contact angle values with tar incorporation in the films. This is desirable for many applications, such as packaging materials where water vapour and oxygen barrier properties are required [27].

Eugenol Release

The drug release profiles of eugenol from tar microparticles and sodium alginate/tar microparticles films were evaluated in aqueous media. Results are presented as cumulative eugenol release as a function of time (Fig. 6). The release profiles showed a controlled release behaviour from all systems. As expected, a higher drug release rate was observed for microparticles suspensions due to the lack of an additional polymeric barrier. For microparticles, the drug release process is mainly influenced

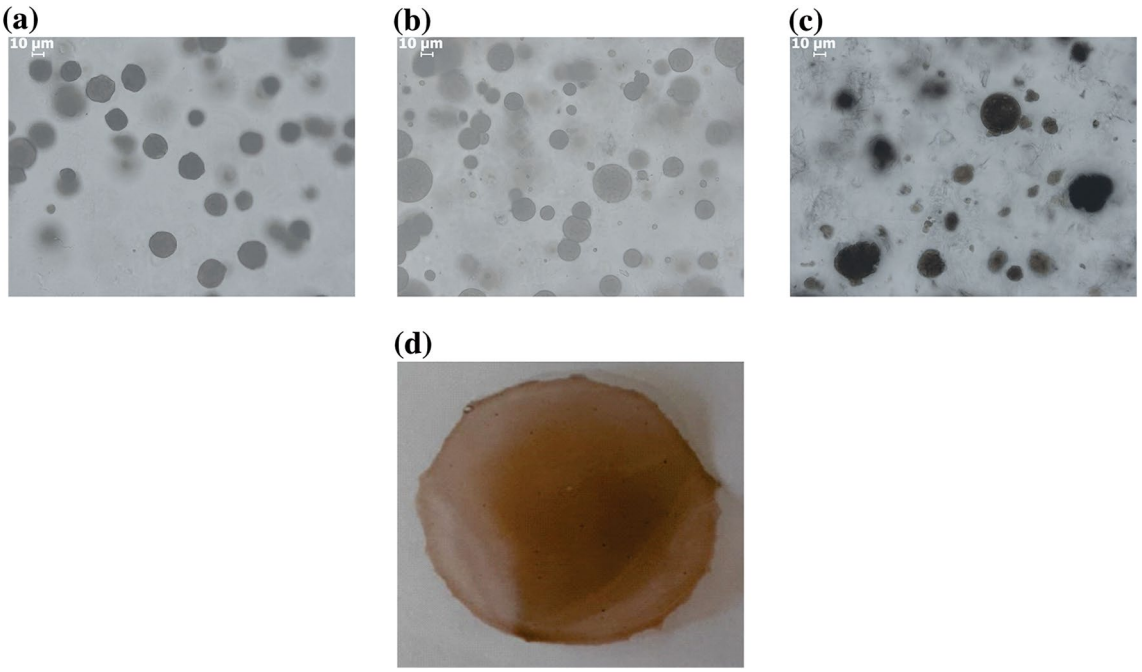

Fig. 3 Optical images of sodium alginate films containing tar microparticles: **a** Alg/Tar, **b** Alg/Tar + $CaCl_2$(20%), **c** Alg/Tar + $CaCl_2$(30%); and **d** photograph of Alg/Tar film

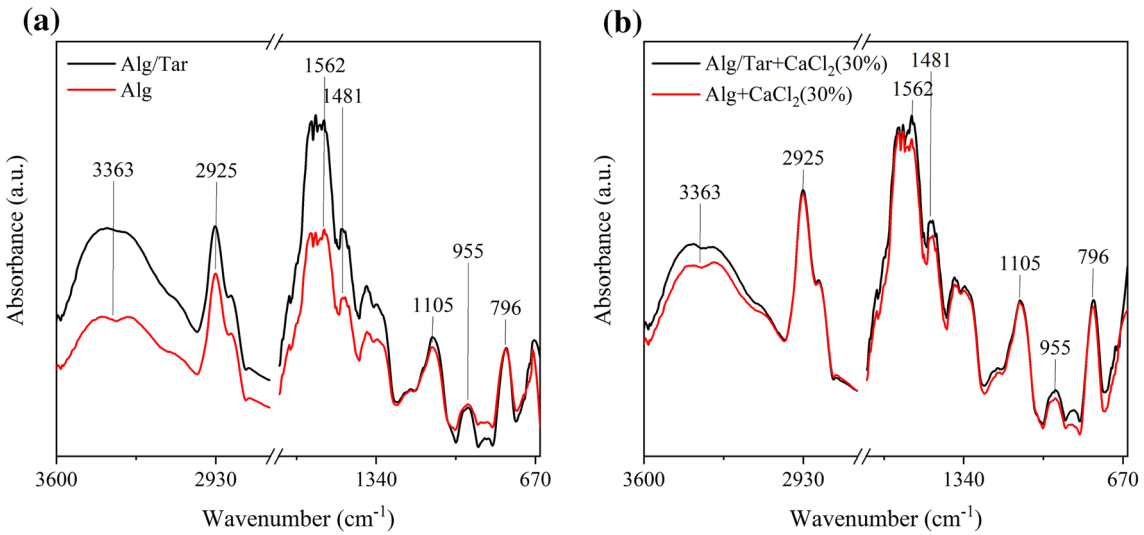

Fig. 4 FTIR spectra of polymeric films: **a** Alg, Alg/Tar; and **b** Alg + $CaCl_2$(30%), Alg/Tar + $CaCl_2$(30%)

by the diffusion of eugenol in the tar matrix. Therefore, particle size is another factor to take into account in the performance of drug release. It is expected that the smaller the size, the faster the eugenol release. The main mechanisms governing the release of eugenol from polymeric films include swelling, drug diffusion and matrix solubilisation. The cumulative eugenol release profile from crosslinked films was significantly different from that of non-crosslinked films because of the lower swelling capacity and solubility of the former. Microparticles suspensions and non-crosslinked films presented a faster initial drug release that was complete after 24 h, while crosslinked formulations showed a slow and sustained release during 72 h approximately. Thus, the crosslinking degree of films is expected to improve the period of eugenol release and the active properties of the films.

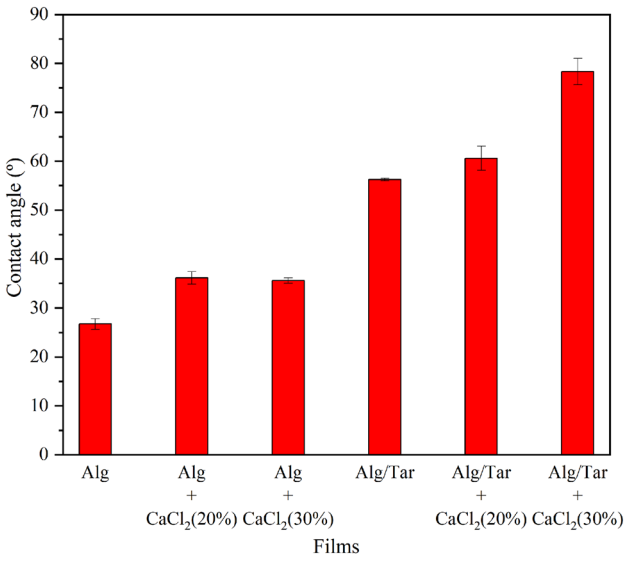

Fig. 5 Contact angle of sodium alginate and sodium alginate-tar films

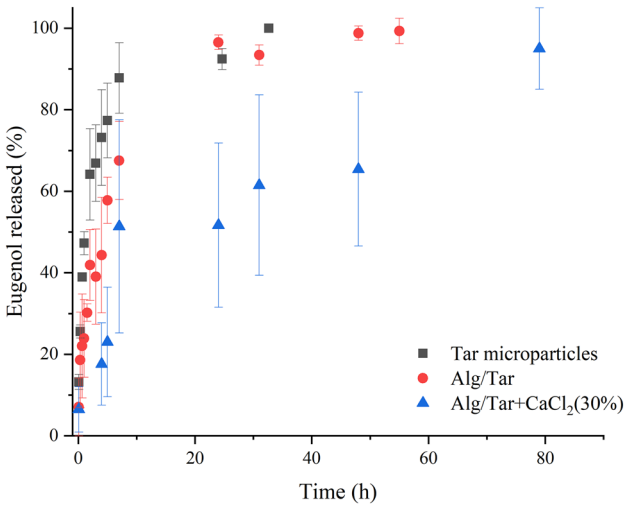

Fig. 6 Eugenol release from different systems: tar microparticles and films Alg/Tar and Alg/Tar + $CaCl_2$(30%)

Antimicrobial Assays

The antimicrobial properties of films containing eugenol-loaded tar microparticles were investigated by the agar diffusion test using *E. coli* and *S. aureus* as representative of gram-negative and gram-positive bacteria, respectively. For comparison purposes, alginate film (A) and alginate film containing non-loaded tar microparticles (B) were also tested as negative controls. The inhibition halos of the films for both microorganisms are presented in Table 5, and an image of an agar plate is shown in Fig. 7 as illustration. As it can be noted, the inhibition halos for *S. aureus* were bigger than those observed for *E. coli*. This behaviour was also reported by Piletti et al. (2017) [28]. The authors attributed the antimicrobial activity of eugenol to the phenolic groups that are very efficient for killing Gram-negative and Gram-positive bacteria. The films containing eugenol-loaded tar microparticles at particle concentrations of 0.3 (C) and 0.6% (D) exhibit noticeable antimicrobial activity.

Table 5 Antimicrobial activity of films by the agar diffusion technique

Microorganism	Zone of inhibition (mm)
S. aureus	C: 13.14 ± 0.38
	D: 17.04 ± 0.38
E. coli	C: 11.54 ± 0.30
	D: 14.33 ± 0.05

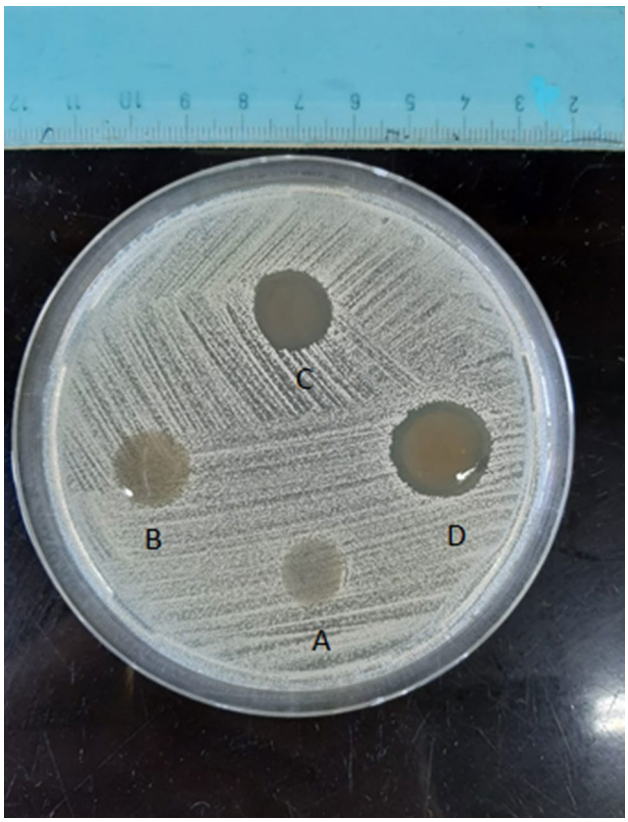

Fig. 7 Example of agar diffusion test using *S. aureus* for: (A) alginate film, (B) alginate film containing non-loaded tar microparticles, (C) alginate film with 0.3% tar microparticles containing eugenol, (D) alginate film with 0.6% tar microparticles containing eugenol

Conclusions

The preparation and characterization of an innovative active packaging material based on alginate film containing tar microparticles loaded with eugenol were studied. The films may help to enhance the shelf life of preserved foods and provide a convenient biodegradable packaging. Moreover, microparticle fabrication provides a novel strategy for the valorization of pyrolytic tar, a subproduct of biomass thermochemical processes. The films exhibited superior thermal, solubility and mechanical properties when $CaCl_2$ was used as a crosslinker agent. The incorporation of tar microparticles in films enhanced their UV barrier properties and surface hydrophobicity, suggesting that the films could be used to protect sensitive food products from light and to form an effective barrier to water. The eugenol release rate was affected by the crosslinking degree of the alginate matrix. Finally, the assessment of the antimicrobial activity of films against two food pathogen bacteria showed that the films containing eugenol-loaded tar microparticles were able to inhibit bacterial growth.

Supplementary Information The online version contains supplementary material available at https://doi.org/10.1007/s12649-022-01679-z.

Acknowledgements The authors are grateful to the Consejo Nacional de Investigaciones Científicas y Técnicas (CONICET), Universidad Nacional del Litoral (U.N.L.), Universidad Tecnológica Nacional (U.T.N.), and Agencia Nacional de Promoción Científica y Tecnológica (ANPCyT) for the financial support.

Author Contributions MET: investigation, formal analysis, data curation, conceptualization, writing—original draft. CB: investigation, formal analysis, data curation, conceptualization, writing—original draft. PS: investigation, formal analysis, writing—original draft. MB: investigation, formal analysis, writing—original draft. US: visualization, conceptualization, writing—review & editing, project administration, funding acquisition. DE: visualization, conceptualization, supervision, writing—review & editing, resources, project administration, funding acquisition.

Funding This work was supported by the Grant N° PIP2011 848 and PUE N° 2920160100007 (CONICET), Grant N° PICT2011 1254 and PICT 1208/2016 (National Agency for Scientific and Technological Promotion (ANPCyT)) and Grant N° CAI+D2011 419 and CAID 50420150100068LI (Universidad Nacional del Litoral).

Data Availability Not applicable.

Code Availability Not applicable.

Declarations

Conflict of interest All authors have read and agreed to the published version of the manuscript.

References

1. Wicochea-Rodríguez, J.D., Chalier, P., Ruiz, T., Gastaldi, E.: Active food packaging based on biopolymers and aroma compounds: how to design and control the release. Front. Chem. **7**, 398 (2019). https://doi.org/10.3389/fchem.2019.00398
2. Barboza, J.N., da Silva Maia Bezerra Filho, C., Silva, R.O., Medeiros, J.V.R., de Sousa, D.P.: An overview on the anti-inflammatory potential and antioxidant profile of eugenol. Oxid. Med. Cell. Longev. (2018). https://doi.org/10.1155/2018/3957262
3. Cheng, J., Wang, H., Kang, S., Xia, L., Jiang, S., Chen, M., Jiang, S.: An active packaging film based on yam starch with eugenol and its application for pork preservation. Food Hydrocoll. **96**, 546–554 (2019). https://doi.org/10.1016/j.foodhyd.2019.06.007
4. Talón, E., Vargas, M., Chiralt, A., González-Martínez, C.: Eugenol incorporation into thermoprocessed starch films using different encapsulating materials. Food Packag. Shelf Life **21**, 100326 (2019). https://doi.org/10.1016/j.fpsl.2019.100326
5. Goñi, M.L., Gañán, N.A., Strumia, M.C., Martini, R.E.: Eugenol-loaded LLDPE films with antioxidant activity by supercritical carbon dioxide impregnation. J. Supercrit. Fluids **111**, 28–35 (2016). https://doi.org/10.1016/j.supflu.2016.01.012
6. Melendez-Rodriguez, B., Figueroa-Lopez, K.J., Bernardos, A., Martínez-Máñez, R., Cabedo, L., Torres-Giner, S., Lagaron, J.M.: Electrospun antimicrobial films of poly(3-hydroxybutyrate-co-3-hydroxyvalerate) containing eugenol essential oil encapsulated in mesoporous silica nanoparticles. Nanomaterials **9**, 227 (2019). https://doi.org/10.3390/nano9020227
7. Purwanti, N., Zehn, A.S., Pusfitasari, D., Khalid, N., Febrianto, Y., Sutrisno, S., Mardjan, A., Kobayashi, I., Zehn, S.: Emulsion stability of clove oil in chitosan and sodium alginate matrix. Int. J. Food Prop. (2018). https://doi.org/10.1080/10942912.2018.1454946
8. Dammak, I., do Sobral, P.J.A.: Active gelatin films incorporated with eugenol nanoemulsions: effect of emulsifier type on films properties. Int. J. Food Sci. Technol. **54**, 2725–2735 (2019). https://doi.org/10.1111/ijfs.14183
9. Rodrigues do Amaral, P.H., Lopes Andrade, P., Costa de Conto, L.: Microencapsulation and its uses in food science and technology: a review (2019). https://doi.org/10.5772/intechopen.81997
10. Wang, S., Wang, Y., Cai, Q., Wang, X., Jin, H., Luo, Z.: Multi-step separation of monophenols and pyrolytic lignins from the water-insoluble phase of bio-oil. Sep. Purif. Technol. **122**, 248–255 (2014). https://doi.org/10.1016/j.seppur.2013.11.017
11. Mullen, C.A., Boateng, A.A.: Characterization of water insoluble solids isolated from various biomass fast pyrolysis oils. J. Anal. Appl. Pyrolysis **90**(2), 197–203 (2011)
12. Zhang, X., Chen, Q., Zhang, Q., Wang, C., Ma, L., Xu, Y.: Conversion of pyrolytic lignin to aromatic hydrocarbons by hydrocracking over pristine MoO_3 catalyst. J. Anal. Appl. Pyrolysis **135**, 60–66 (2018). https://doi.org/10.1016/j.jaap.2018.09.020
13. Wang, C., Li, M., Fang, Y.: Upgrading of pyrolytic lignin into hexamethylbenzene with high purity: demonstration of the "all-to-one" biochemical production strategy in thermo-chemical conversion. Green Chem. **21**, 1000–1005 (2019). https://doi.org/10.1039/c8gc03788d
14. Zhang, L., Zhang, S., Hu, X., Gholizadeh, M.: Progress in application of the pyrolytic lignin from pyrolysis of biomass. Chem. Eng. J. (2021). https://doi.org/10.1016/j.cej.2021.129560
15. Garcia-Perez, M., Chaala, A., Pakdel, H., Kretschmer, D., Roy, C.: Characterization of bio-oils in chemical families. Biomass Bioenergy **31**(4), 222–242 (2007)

16. Zhang, X., Zhu, J., Wu, C., Wu, Q., Liu, K., Jiang, K.: Preparation and properties of wood tar-based rejuvenated asphalt. Materials (Basel) (2020). https://doi.org/10.3390/ma13051123
17. Tian, X., Zhang, L., Li, H., Zhang, X., Wang, Q., Jin, L., Cao, Q.: Preparation of bio-oil-based polymer microspheres for adsorption Cu^{2+} and its adsorption behaviors. J. Dispers. Sci. Technol. (2020). https://doi.org/10.1080/01932691.2020.1727344
18. Liakos, I., Rizzello, L., Scurr, D.J., Pompa, P.P., Bayer, I.S., Athanassiou, A.: All-natural composite wound dressing films of essential oils encapsulated in sodium alginate with antimicrobial properties. Int. J. Pharm. **463**, 137–145 (2014). https://doi.org/10.1016/j.ijpharm.2013.10.046
19. Aadil, K.R., Prajapati, D., Jha, H.: Improvement of physcio-chemical and functional properties of alginate film by Acacia lignin. Food Packag. Shelf Life **10**, 25–33 (2017). https://doi.org/10.1016/j.fpsl.2016.09.002
20. Mauriello, G., Ercolini, D., La Storia, A., Casaburi, A., Villani, F.: Development of polythene films for food packaging activated with an antilisterial bacteriocin from *Lactobacillus curvatus* 32Y. J. Appl. Microbiol. **97**, 314–322 (2004). https://doi.org/10.1111/j.1365-2672.2004.02299.x
21. Prauchner, M.J., Pasa, V.M.D., Otani, C., Otani, S.: Characterization and thermal polymerization of *Eucalyptus* tar pitches. Energy Fuels **15**, 449–454 (2001). https://doi.org/10.1021/ef000196o
22. Simões, M.G., Coimbra, P.A., Carreira, S., Figueiredo, M.M., Gil, M.H., Simões, P.N., Simões, M.G.: Eugenol-loaded microspheres incorporated into textile substrates. Cellulose **27**, 4109–4121 (2020). https://doi.org/10.1007/s10570-020-03010-2
23. Michelin, M., Marques, A.M., Pastrana, L.M., Teixeira, J.A., Cerqueira, M.A.: Carboxymethyl cellulose-based films: effect of organosolv lignin incorporation on physicochemical and antioxidant properties. J. Food Eng. **285**, 110107 (2020). https://doi.org/10.1016/j.jfoodeng.2020.110107
24. Xiao, C., Weng, L., Zhang, L.: Improvement of physical properties of crosslinked alginate and carboxymethyl konjac glucomannan blend films. J. Appl. Polym. Sci. **84**, 2554–2560 (2002). https://doi.org/10.1002/app.10582
25. Tavares, L.B., Ito, N.M., Salvadori, M.C., dos Santos, D.J., Rosa, D.S.: PBAT/kraft lignin blend in flexible laminated food packaging: peeling resistance and thermal degradability. Polym. Test. **67**, 169–176 (2018). https://doi.org/10.1016/j.polymertesting.2018.03.004
26. Campos-Vallette, M.M., Chandía, N.P., Clavijo, E., Leal, D., Matsuhiro, B., Osorio-Román, I.O., Román, R., Torres, S.: Characterization of sodium alginate and its block fractions by surface-enhanced Raman spectroscopy. J. Raman Spectrosc. (2010). https://doi.org/10.1002/jrs.2517
27. Teno, J., González-Gaitano, G., González-Benito, J.: Poly(ethylene-co-vinyl acetate) films prepared by solution blow spinning: surface characterization and its relation with *E. coli* adhesion. Polym. Test. **60**, 140–148 (2017). https://doi.org/10.1016/j.polymertesting.2017.03.020
28. Piletti, R., Bugiereck, A.M., Pereira, A.T., Gussati, E., Dal Magro, J., Mello, J.M.M., Dalcanton, F., Ternus, R.Z., Soares, C., Riella, H.G., Fiori, M.A.: Microencapsulation of eugenol molecules by β-cyclodextrine as a thermal protection method of antibacterial action. Mater. Sci. Eng. C **75**, 259–271 (2017). https://doi.org/10.1016/j.msec.2017.02.075